PROCEEDINGS OF SCIENCE

Squark production with R-symmetry beyond NLO at the LHC

Wojciech Kotlarski,[a,*] **Christoph Borschensky,**[b] **Fausto Frisenna, Jan Kalinowski,**[c] **Anna Kulesza**[d] **and Dominik Stöckinger**[e]

[a] *National Centre for Nuclear Research, Pasteura 7, 02-093 Warsaw, Poland*
[b] *Institute for Theoretical Physics, Karlsruhe Institute of Technology, Wolfgang-Gaede-Str. 1, 76131 Karlsruhe, Germany*
[c] *Faculty of Physics, University of Warsaw, Pasteura 5, 02-093 Warsaw, Poland*
[d] *Institute for Theoretical Physics, University of Münster, Wilhelm-Klemm-Straße 9, 48149 Münster, Germany*
[e] *Institut für Kern- und Teilchenphysik, Zellescher Weg 19, 01069 Dresden, Germany*
E-mail: wojciech.kotlarski@ncbj.gov.pl, christoph.borschensky@kit.edu, jan.kalinowski@fuw.edu.pl, anna.kulesza@uni-muenster.de, dominik.stoeckinger@tu-dresden.de

We summarize recent developments in the analysis of the SQCD sector of the Minimal R-symmetric Supersymmetric Standard Model (MRSSM). This model allows to evade direct collider limits on squark masses from the MSSM and presents an opportunity to study unusual BSM features like Dirac gluinos and colour-octet scalars. We review MRSSM phenomenology, its collider limits and improvements to the accuracy of MRSSM predictions for the LHC: the evaluation of next-to-leading order SQCD corrections to squark-(anti-)squark pair production and the recent threshold resummation of soft gluon corrections to these processes.

Proceedings of the Corfu Summer Institute 2024 "School and Workshops on Elementary Particle Physics and Gravity" (CORFU2024) 12 - 26 May, and 25 August – 27 September, 2024
Corfu, Greece

*Speaker

 ISSN 1824-8039 . Published by SISSA Medialab.

PoS(CORFU2024)392

1. Introduction

The search at Large Hadron Collider (LHC) for colour-charged signals from the Beyond the Standard Model (BSM) physics has over the last decade pushed mass limits for some of postulated new states to well above 1 TeV. This has led to the perception that, should BSM physics exist at all, only light electroweak states remain permissible. Such limits are, however, much less model independent than one might initially assume. For instance, in supersymmetry, the data gathered at the LHC is typically analysed within the Minimal Supersymmetric Standard Model (MSSM), along with its simplified versions and derivatives. Although some electroweak (EW) extensions of the MSSM are occasionally examined (such as the Next-to-Minimal Supersymmetric Standard Model), SUSY QCD (SQCD) extensions are rarely investigated beyond SUSY-inspired simplified models. This represents a considerable oversight in current SUSY searches, as the limits in various SQCD extensions can differ significantly.

A notable category of often overlooked SUSY models includes various models with Dirac gluinos. Such models cannot be approximated by the MSSM. They enhance gluino production but exhibit a significant suppression of squark-squark production cross-sections [1–3], which are the primary channels responsible for squark mass exclusions. This significantly diminishes the mass limits on first few generations of squarks [1, 4], rendering these models feasible in scenarios where a corresponding MSSM model would face experimental exclusion.

Simultaneously, numerous comprehensive models that incorporate Dirac gluinos present intriguing opportunities for investigation of EW signatures due to their extended EW sectors. One such model is the supersymmetric variant of the Standard Model (SM) characterized by an unbroken R-symmetry [5, 6]. R-symmetry forbids Majorana mass terms leading to the introduction of Dirac gauginos if the model is to be phenomenologically viable. The simplest realization of this concept, the Minimal R-symmetric Supersymmetric Standard Model (MRSSM) [7], has undergone extensive analysis in recent years. This model has been shown to agree with measurements of Higgs boson properties [8–10], dark matter [10, 11], constraints on the muon $g-2$ [12], predictions regarding the mass of the W-boson [8, 13], and it also offers promising avenues for forthcoming lepton flavour violation experiments [12].

In the context of the LHC it has been shown that a realistic experimental analysis of the MRSSM SQCD sector, incorporating detector effects and next-to-leading (NLO) corrections to squark-(anti-)squark production performed in Ref. [4] confirms findings of Ref. [1]. Further improvement to the accuracy of this analysis was the incorporation of threshold resummation of soft-gluon corrections at the the next-to-next-to-leading-logarithmic level (NNLL) for the $\tilde{q}\tilde{q}^*$ process and at the next-to-leading-logarithmic (NLL) level for the $\tilde{q}\tilde{q}$ [3].

In this note we summarize all of the above mentioned findings. In Sec. 2 we briefly discuss the construction of the MRSSM, with an emphasis on its strongly interacting sector. In Sec. 3 we review the phenomenology of the MRSSM: the SQCD collider limits, discuss the evaluation of next-to-leading-order corrections and threshold resummation of soft gluon corrections to squark production. We summarize our findings in Sec. 4.

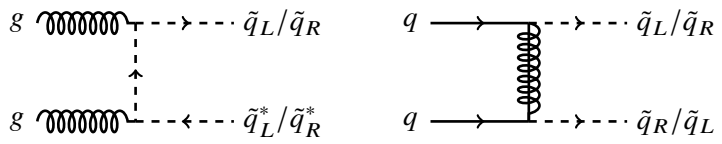

Figure 1: Examples of tree-level diagrams contributing to the production of squark-antisquark and squark-squark pairs. The second diagram exemplifies t-channel gluino exchange, where in the MRSSM only the two indicated chirality combinations of squarks are possible because of R-charge conservation.

2. SQCD sector of the Minimal R-symmetric supersymmetric Standard Model

The MRSSM is distinct from the popular SUSY models like the MSSM and the NMSSM by featuring an exact, global $U(1)$ R-symmetry [5, 6] under which SM fields and their superpartners have different charges. One of an important phenomenological consequences of that symmetry is that left-right sfermion mixing and Majorana mass terms for gauginos are forbidden. While the lack of mixing protects flavour observables, the presence of massles gauginos is clearly experimentally excluded. For every gauge group factor the model therefore introduces a chiral multiplet providing degrees of freedom necessary to construct Dirac gauginos, for which mass terms are allowed by the symmetry.

The strongly interacting sector of the MRSSM is summarized as follows:

- For each quark flavour q_i, there is a "left-handed" squark $\tilde{q}_{iL}$ with R-charge $R = +1$ and a "right-handed" squark $\tilde{q}_{iR}$ with R-charge $R = 1$. Squarks of different type cannot mix, in contrast to the MSSM, but flavour mixing is possible.

- The gluino is a Dirac fermion with R-charge $R = +1$. Its left-handed component behaves like the MSSM gluino and is the superpartner of the gluon, contained in a vector superfield. The right-handed gluino component is part of an additional antichiral supermultiplet having no direct couplings to quarks or squarks.

- The model contains a scalar gluon (sgluon) field with R-charge $R = 0$. The gluon, gluino and the sgluon together form an $N = 2$ SUSY multiplet. The CP-components of the complex sgluon field are split by the D-term contribution as $O = (O_s + iO_p)/\sqrt{2}$, with the tree-level masses given by $m_{O_p} = m_O$ and $m^2_{O_s} = m^2_O + 4m^2_{\tilde{g}}$.

The structure of the model, its mass matrices and β functions motivate scenarios in which the squarks are the lightest coloured SUSY particles — significantly lighter than gluinos. However, due to the constraints imposed by R-symmetry, the model also has a potential to evade their experimental detection.

3. Phenomenological implications of R-symmetry in the squark sector

In Fig. 1 we show example diagrams contributing to squark-squark and squark-antisquark production in the MRSSM. At the tree-level, the squark production cross-sections in this model are

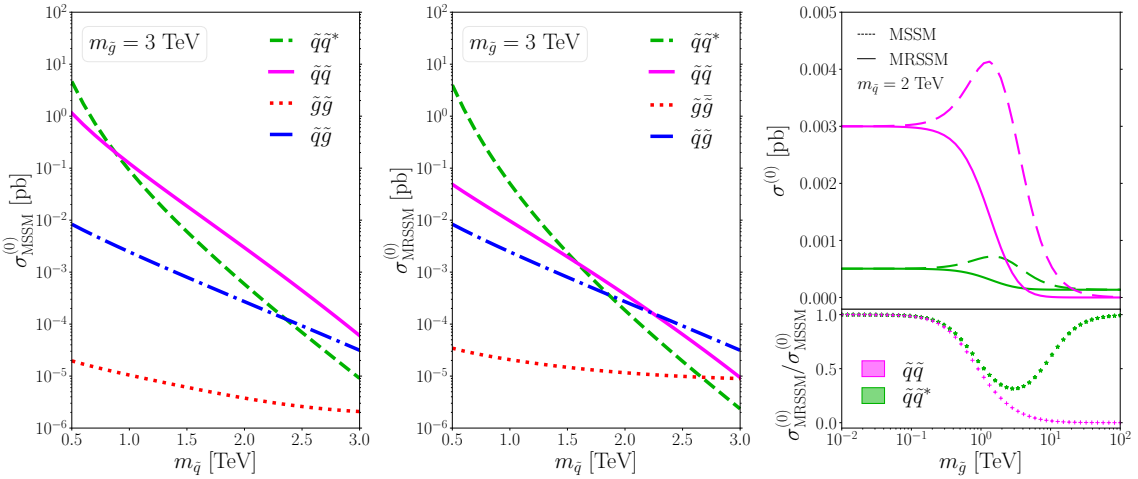

Figure 2: LO cross sections at the LHC for $\sqrt{S} = 13.6$ TeV, summed over the first five flavours. Left plot: gluino and squark production in the MSSM at fixed $m_{\tilde{g}} = 3$ TeV. Center: equivalent processes in the MRSSM. Right: squark production across a wide gluino mass range, having fixed $m_{\tilde{q}} = 2$ TeV.

given by

$$\begin{aligned}\hat{\sigma}^B(q_i\overline{q}_j \to \tilde{q}\tilde{q}^\dagger) &= \delta_{ij}\frac{g_s^4}{16\pi\hat{s}}(n_f-1)\left[\frac{4}{27}-\frac{16m_{\tilde{q}}^2}{27\hat{s}}\right]\beta_{\tilde{q}} \\ &+ \delta_{ij}\frac{g_s^2\hat{g}_s^2}{16\pi\hat{s}}\left[\left(\frac{4}{27}+\frac{8m_-^2}{27\hat{s}}\right)\beta_{\tilde{q}}+\left(\frac{8m_{\tilde{g}}^2}{27\hat{s}}+\frac{8m_-^4}{27\hat{s}^2}\right)L_1\right] \\ &+ \frac{\hat{g}_s^4}{16\pi\hat{s}}\left[-\frac{8}{9}\beta_{\tilde{q}}+\left(-\frac{4}{9}-\frac{8m_-^2}{9\hat{s}}\right)L_1\right], \qquad (1)\end{aligned}$$

$$\hat{\sigma}^B(gg \to \tilde{q}\tilde{q}^\dagger) = \frac{(n_f-1)g_s^4}{16\pi\hat{s}}\left[\left(\frac{5}{24}+\frac{31m_{\tilde{q}}^2}{12\hat{s}}\right)\beta_{\tilde{q}}+\left(\frac{4m_{\tilde{q}}^2}{3\hat{s}}+\frac{m_{\tilde{q}}^4}{3\hat{s}^2}\right)\ln\frac{1-\beta_{\tilde{q}}}{1+\beta_{\tilde{q}}}\right], \qquad (2)$$

$$\hat{\sigma}^B(q_iq_j \to \tilde{q}\tilde{q}) = \frac{\hat{g}_s^4}{16\pi\hat{s}}\left[-\frac{8}{9}\beta_{\tilde{q}}+\left(-\frac{4}{9}-\frac{8m_-^2}{9\hat{s}}\right)L_1\right], \qquad (3)$$

where $\hat{s}$ is the squared partonic centre-of-mass energy and

$$\beta_{\tilde{q}} \equiv \sqrt{1-\frac{4m_{\tilde{q}}^2}{\hat{s}}}, \qquad m_-^2 \equiv m_{\tilde{g}}^2 - m_{\tilde{q}}^2, \qquad L_1 = \ln\frac{\hat{s}+2m_-^2-\hat{s}\beta_{\tilde{q}}}{\hat{s}+2m_-^2+\hat{s}\beta_{\tilde{q}}}.$$

Of special importance in the MRSSM is the squark-squark production. For the allowed channels in the MRSSM, the chirality projectors lead to the following replacement

$$\frac{\not{p}+m_{\tilde{g}}}{p^2-m_{\tilde{g}}^2} \to \frac{\not{p}}{p^2-m_{\tilde{g}}^2} \qquad (4)$$

for the gluino propagator in the right diagram in Figure 1. On the level of the cross section, compared to the MSSM, this manifests in the substitution

$$\frac{\hat{g}_s^4}{16\pi^2\hat{s}}\left(-\frac{4}{9}-\frac{4m_-^4}{9(m_{\tilde{g}}^2\hat{s}+m_-^4)}\right)\beta_{\tilde{q}} \to -\frac{\hat{g}_s^4}{16\pi^2\hat{s}}\cdot\frac{8}{9}\beta_{\tilde{q}}, \tag{5}$$

and the vanishing of the term proportional to gluino mass in both nominator and denominator of $\tilde{q}\tilde{q}$ production compared to the MSSM expressions. Expanding $\hat{\sigma}^B(q_iq_j \to \tilde{q}\tilde{q})$ in $m_{\tilde{g}}$ shows that the leading term in the MSSM is proportional to $m_{\tilde{g}}^{-2}$, whereas in the MRSSM it is $m_{\tilde{g}}^{-4}$, as expected from Eq. (4).

Figure 2 compares predicted squark and gluino production cross sections between the MSSM and the MRSSM in function of squark and gluino masses at the 13.6 TeV LHC. The $\tilde{q}\tilde{q}^*$ cross sections remains mostly unaltered. The biggest difference is observed in the $\tilde{q}\tilde{q}$ and $\tilde{g}\tilde{g}$ production. The $\tilde{q}\tilde{q}$ production drops significantly, while the gluino cross section increases by roughly a factor of 2. The dependence on the gluino mass, discussed around Eq. (5), is illustrated in the right panel of Fig. 2. For small gluino masses, both cross sections in both models are roughly identical. For very large gluino masses, the $\tilde{q}\tilde{q}^*$ cross section become similar again, though the $\tilde{q}\tilde{q}$ drops much faster in the MRSSM than in the MSSM. This significantly lowers the squark exclusion limits from the LHC.

These observations motivated the interest in the study of those processes in the MRSSM. However, a sensible comparison against current MSSM analyses and against the experimental data calls for the inclusion of higher order corrections.

The calculation of NLO corrections for squark production in the MRSSM was performed in two independent ways [2]. The first calculation was conducted within the MadGraph5_aMC@NLO framework, with virtual matrix elements provided by GoSam supplemented with hand coded renormalization constants and utilizing the Frixione, Kunszt and Signer method for the subtraction of soft/collinear divergences. The second one was based on semi-analytical FeynArts/FormCalc calculation employing the two-cut phase space slicing technique for the treatment of IR divergences.

For $\tilde{q}\tilde{q}$ production, the total NLO contributions can decrease the LO cross section by 10% and can increase them by more than 50% assuming sgluons are close in mass to gluino and squarks (Fig. 3). The relative size of the corrections falls with rising gluino mass while increasing squark masses lead to an enhancement. This feature is already present in the MSSM and not influenced by the Dirac nature of the gluino or the presence of the sgluon. In the scenario of interest, with a heavy Dirac gluino and rather light squarks, the size of NLO corrections is reduced compared to the remainder of the parameter space. The K-factors for $\tilde{q}\tilde{q}^*$ production are in general smaller than the ones for the $\tilde{q}\tilde{q}$ production. They reach up to 30%. The corrections are largest for small squark and gluino masses. For small squark masses, the gluino mass does not influence the K-factor significantly. In this region pure QCD corrections are dominant and only with a large sgluon mass do the non-decoupling effect of sgluon become important. The K-factor is smallest for large squark masses and increases in this parameter region with the gluino mass. The MRSSM K-factors are higher and dependent on the hierarchy between squark, gluino and sgluon masses and should be taken into account to obtain valid limits. On the other hand, our NLO results show that the assumption that the K-factors in the MSSM and MRSSM are equal is not correct.

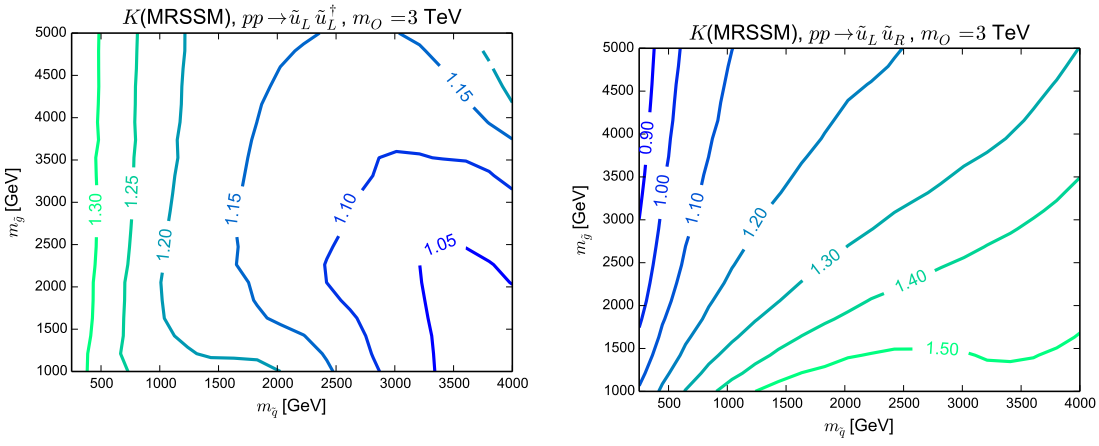

(a) **(b)**

Figure 3: MRSSM K-factors for $\tilde{u}_L \tilde{u}_L^*$ (a) and $\tilde{u}_L \tilde{u}_R$ (b) production at 13 TeV LHC for octet mass of 3 TeV.

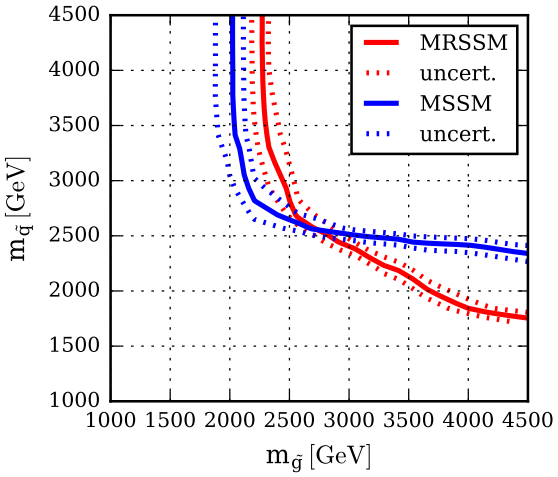

Figure 4: Mass limits on squarks and gluinos in case of degenerate 1st and 2nd generation squarks. The limits are based on a recasting of LHC analyses as explained in [4].

Based on the NLO calculation we derived bounds on squark and gluino masses from LHC searches, as were available in 2016–2017 (see Ref. [4] for a list of used experimental analysis). Figure 2 shows the exclusion contours in the squark–gluino mass plane for the MRSSM and the MSSM. The figure showcases the trade off between exclusions for squark and gluino masses, where heavy gluino allows for lighter squarks in the MRSSM while light gluinos are excluded.

Further refinement to MRSSM predictions is the resummation of the soft-gluon contributions. The resummation of the soft-gluon contributions is performed after taking a Mellin transform (in-

dicated by a tilde) of the hadronic cross section,

$$\tilde{\sigma}_{h_1h_2\to\tilde{q}\tilde{q}^{(*)}}(N) \equiv \int_0^1 d\rho\ \rho^{N-1}\ \sigma_{h_1h_2\to\tilde{q}\tilde{q}^{(*)}}(\rho) = \sum_{i,j} \tilde{f}_{i/h_1}(N+1,\mu^2)\,\tilde{f}_{j/h_2}(N+1,\mu^2)\,\tilde{\hat{\sigma}}_{ij\to\tilde{q}\tilde{q}^{(*)}}(N,\mu^2)\,, \tag{6}$$

where ρ is a hadronic threshold variable, $\rho = 4m_{\tilde{q}}^2/S$. Partonic quantities are indicated by a hat symbol. The logarithmic contributions become large when the partonic centre-of-mass energy $\sqrt{\hat{s}}$ approaches $2m_{\tilde{q}}$, i.e. in this limit, the partonic threshold variable $\hat{\rho} = 4m_{\tilde{q}}^2/\hat{s}$ behaves as $\hat{\rho} \to 1$. The corresponding limit in Mellin space is $N \to \infty$.

The hadronic cross section $\sigma_{h_1h_2\to\tilde{q}\tilde{q}^{(*)}}$ in physical momentum space can be obtained by performing the inverse Mellin transform. To retain full information contained in the complete NLO cross section [2], we combine the NLO and NNLL results through a matching procedure that avoids double counting of the NLO terms:

$$\sigma^{(\mathrm{NLO+(N)NLL})}_{h_1h_2\to\tilde{q}\tilde{q}^{(*)}}(\rho,\mu^2) = \sum_{i,j}\int_{\mathrm{CT}}\frac{dN}{2\pi\mathrm{i}}\,\rho^{-N}\,\tilde{f}_{i/h_1}(N+1,\mu^2)\tilde{f}_{j/h_2}(N+1,\mu^2) \times\left[\tilde{\hat{\sigma}}^{(\mathrm{res})}_{ij\to\tilde{q}\tilde{q}^{(*)}}(N,\mu^2) - \tilde{\hat{\sigma}}^{(\mathrm{res})}_{ij\to\tilde{q}\tilde{q}^{(*)}}(N,\mu^2)\Big|_{(\mathrm{NLO})}\right] + \sigma^{(\mathrm{NLO})}_{h_1h_2\to\tilde{q}\tilde{q}^{(*)}}(\rho,\mu^2), \tag{7}$$

where "res" refers to either NNLL or NLL.

The all-order summation of logarithmic terms is based on the factorisation of the hard, (soft)-collinear, and wide-angle soft modes in the cross section. Near threshold, the resummed partonic cross section up to NNLL accuracy has the form:

$$\tilde{\hat{\sigma}}^{(\mathrm{res})}_{ij\to\tilde{q}\tilde{q}^{(*)}}(N,\mu^2) = \sum_I \tilde{\hat{\sigma}}^{(0)}_{ij\to\tilde{q}\tilde{q}^{(*)},I}(N,\mu^2)\,\left(1+\frac{\alpha_\mathrm{s}}{\pi}\,C^{(1)}_{ij\to\tilde{q}\tilde{q}^{(*)},I}(N,\mu^2)\right) \times\exp\left[Lg_1(\alpha_\mathrm{s}L)+g_{2,I}(\alpha_\mathrm{s}L)+\alpha_\mathrm{s}g_{3,I}(\alpha_\mathrm{s}L)\right], \tag{8}$$

where $\tilde{\sigma}^{(0)}_{ij\to\tilde{q}\tilde{q}^{(*)},I}$ denotes the colour-decomposed LO cross section in Mellin-moment space. The colour label I corresponds to an irreducible representation of the colour structure of the process. The one-loop matching coefficient $C^{(1)}_{ij\to\tilde{q}\tilde{q}^{(*)},I}$ collects all $O(\alpha_\mathrm{s}^3)$ non-logarithmic (in N) contributions which do not vanish at threshold. The exponent in the second line of Eq. (8) captures all dependence on the large logarithm $L = \log(N)$. Reaching the NLL accuracy requires knowledge of the g_1 and g_2 functions in the exponential. The NNLL accuracy additionally requires knowledge of g_3, as well as the one-loop matching coefficient $C^{(1)}$ which is not included at NLL. While the exponential factor in Eq. (8) is the same as in the case of the MSSM and the functions g_i are well known, the calculation of $C^{(1)}$ needs to be carried out anew for the MRSSM [3].

To study the effect of N(N)LL resummation, we define a resummation K-factors $K_{(\mathrm{N})\mathrm{NLL}}$ as

$$K_{(\mathrm{N})\mathrm{NLL}} \equiv \frac{\sigma^{\mathrm{NLO+(N)NLL}}}{\sigma^{\mathrm{NLO}}}\,. \tag{9}$$

Figure 5 shows a K_{NNLL} for the $\tilde{q}\tilde{q}^*$ and K_{NLL} for $\tilde{q}\tilde{q}$ production for the octet soft mass of m_O = 2 TeV. The accuracy of resummation is different for the two processes due to the difference in the

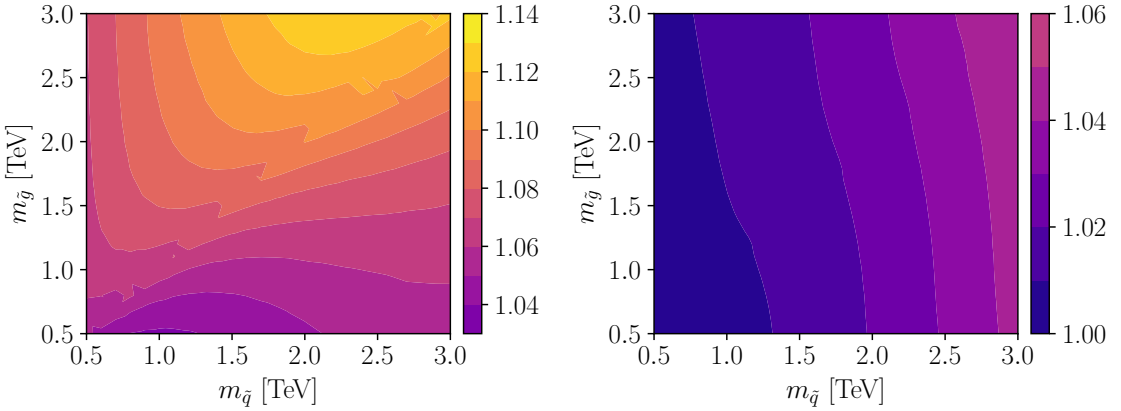

Figure 5: K_{NNLL} factors for $\tilde{q}\tilde{q}^*$ production (left column) and K_{NLL} factors for $\tilde{q}\tilde{q}$ production (right column) for $m_O = 2$ TeV, as defined in Eq. (9). Results for $m_O = 100$ TeV look broadly the same.

composition of the cross section in terms of partial waves. It reaches NLO+NNLL for the $\tilde{q}\tilde{q}^*$ process, while the $\tilde{q}\tilde{q}$ production is considered at NLO+NLL. As expected, we see that soft-gluon corrections get larger with increasing squark masses. The NNLL corrections can increase the $\tilde{q}\tilde{q}^*$ cross section by up to 14%. For $\tilde{q}\tilde{q}$ production in the MRSSM, with the dominant contribution to the LO cross section in the p-wave channel and consequently, the resummed correction being only of NLL order, the change in the cross section amounts to at most a few per cent for $m_{\tilde{q}}$ and $m_{\tilde{g}}$ up to 3 TeV. The relative soft-gluon corrections to the $\tilde{q}\tilde{q}$ and $\tilde{q}\tilde{q}^*$ MRSSM cross sections do not significantly depend on the sgluon mass, in agreement with the sgluon mass only entering in the genuine one-loop diagrams.

The MRSSM and the MSSM K-factors for the $\tilde{q}\tilde{q}^*$ process differ substantially in their dependence on the gluino mass. While the $\tilde{q}\tilde{q}^*$ MSSM K-factor depends weekly on $m_{\tilde{g}}$, the MRSSM K-factor has a stronger dependence on $m_{\tilde{g}}$ than on $m_{\tilde{q}}$. At NNLL, the MRSSM correction grows with $m_{\tilde{g}}$ and a correction of comparable size to the one in the MSSM only when the gluino mass is sufficiently high. The N(N)LL K-factors are shown in Fig. 5.

The advertised suppression of squark cross sections compared to the MSSM persists beyond the NLO level. In Fig. 6 we show the ratios of MRSSM to MSSM cross-sections in the squark mass – gluino mass plane computed at the highest possible common accuracy. Squark-antisquark cross-sections are computed at NLO+NNLL (top row), while squark-squark ones at NLO+NLL (bottom row). The plots are shown for two selected sgluons masses, 2 (left column) and 100 TeV (right column).

Apart from modifying the predictions for the total cross sections, threshold corrections also reduce the theoretical uncertainty. Using 3-point scale variation as a proxy for missing higher order contributions we observe reduction of renormalization scale uncertainty, particularly for the $\tilde{q}\tilde{q}^*$ production, as shown in Fig. 7. The factorisation scale uncertainty is reduced to a smaller extent, which is visible mostly for large squark and gluino masses.

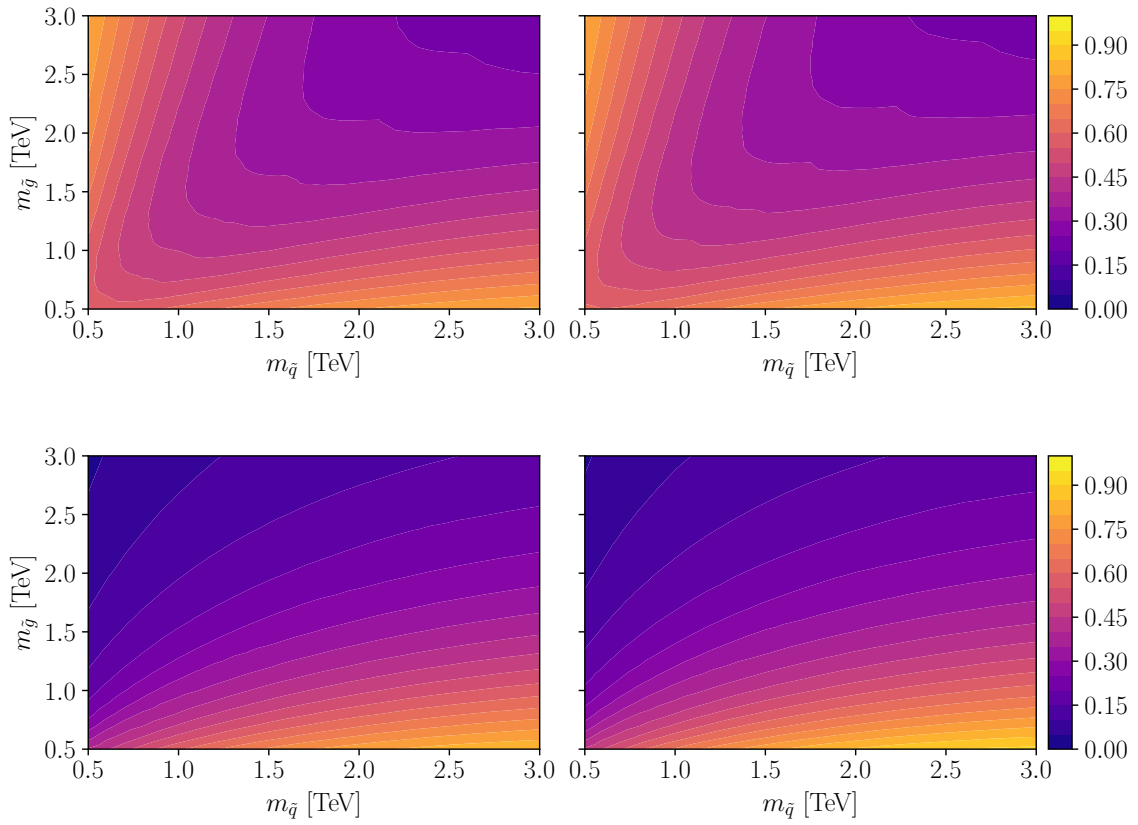

Figure 6: Ratios of MRSSM cross sections over the MSSM ones, computed at the same accuracy. For $\tilde{q}\tilde{q}^*$ production (top row), the cross sections are calculated at NLO+NNLL, while for $\tilde{q}\tilde{q}$ production (bottom row), the calculation is performed at NLO+NLL. The ratios are shown for two sgluon mass configurations for the MRSSM predictions: $m_O = 2$ TeV (left column), and $m_O = 100$ TeV (right column).

4. Conclusions

The Minimal R-symmetric Supersymmetric Standard Model (MRSSM) is an interesting alternative candidate for a supersymmetrized Standard Model. Its defining feature is its unbroken, global R-symmetry. The symmetry, initially adopted for its capacity to protect a SUSY model from flavour constraints even in the presence of large flavour-violating terms in sfermion mass matrices, results also in an extraordinarily rich phenomenology in various other sectors leading to a distinct low, EW and TeV-scale predictions.

A notable consequence of R-symmetry is the emergence of a Dirac gluino, which leads to a reduction of squark-squark production cross-sections — the primary factor driving squark mass limits at hadron colliders. This significantly diminishes the limits on squark masses at the cost of increasing the limit on the gluino mass, thereby reducing the mass gap between the Standard Model and superpartners in the electroweak sector. It renders the model more natural and modifies the conventional MSSM-like squark-gluino mass plane exclusion regions. This is the source of interest in the super-QCD phenomenology of this model at the LHC.

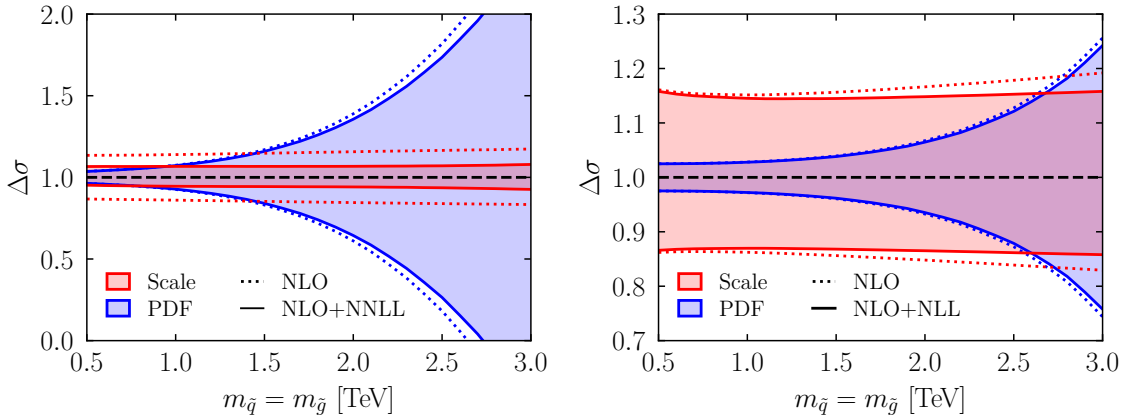

Figure 7: Scale and PDF+α_s uncertainties for $\tilde{q}\tilde{q}^*$ production at NLO+NNLL (left) and $\tilde{q}\tilde{q}$ production at NLO+NLL (right) in the MRSSM, with the sgluon mass being fixed to $m_O = 100$ TeV. $\Delta\sigma$ is defined as the relative uncertainty with respect to the central cross-section prediction. The scale uncertainty shown here is obtained via the 3-point method.

Motivated by this findings, in this note we have reviewed the progress in deriving precise constraints on squark masses within the MRSSM. We detailed the computation of next-to-leading order SQCD corrections to squark-(anti-)squark pair production based on two independent calculations. The first calculation was conducted within the MadGraph5_aMC@NLO framework, with virtual matrix elements provided by GoSam supplemented with hand coded renormalization constants and utilizing the Frixione, Kunszt and Signer method for the subtraction of soft/collinear divergences. The second one was based on semi-analytical FeynArts/FormCalc calculation employing the two-cut phase space slicing technique for the treatment of IR divergences. The NLO corrections give a moderate K-factor and significantly reduce the theoretical uncertainty associated with squark pair production. Moreover, they render the prediction sensitive to parameters such as sgluon masses, which could only be investigated through direct sgluon production at the LHC in the past. The sgluon demonstrates a non-decoupling effect on squark pair production, making the process sensitive to sgluon masses to well beyond the kinematic limit for direct sgluons production at the LHC.

The NLO predictions were confronted with experimental data using Monte Carlo simulation and simplified parametrization of detector response. We obtained substantially weaker limits on squark masses compared to the MSSM: for simple scenarios with heavy gluinos and degenerate squarks the MRSSM mass limit, based on the data available at the time of the analysis, was $m_{\tilde{q}} > 1.7$ TeV — approximately 600 GeV lower than in the MSSM.

The remaining theoretical uncertainty was further reduced by applying threshold resummation of soft-gluon corrections at the next-to-next-to-leading-logarithmic (NNLL) level for the $\tilde{q}\tilde{q}^*$ process and at the next-to-leading-logarithmic (NLL) level for the $\tilde{q}\tilde{q}$ process (since in the later case the dominant contribution to the LO cross section is in the p-wave channel). The (N)NLL k-factors were generally found to be small, up to ~15% for $\tilde{q}\tilde{q}^*$ and ~5% for $\tilde{q}\tilde{q}$ in extreme cases, assuming we limit ourself to $m_{\tilde{g}}$ and $m_{\tilde{q}}$ being less than 3 TeV. This confirmed the reliability of the previously obtained NLO results and the collider constraints derived from them.

While the $\tilde{q}\tilde{q}$ MSSM K-factor almost does not depend on $m_{\tilde{g}}$, the MRSSM K-factor appears to have a stronger dependence on $m_{\tilde{g}}$ than on $m_{\tilde{q}}$. We observed that the relative soft-gluon corrections to the $\tilde{q}\tilde{q}$ and $\tilde{q}\tilde{q}^*$ MRSSM cross sections do not significantly depend on the sgluon mass as it only appears in the one-loop diagrams.

Acknowledgements

We thank Philip Diessner and Sebastian Liebschner for their collaboration during various stages of this project.

WK is supported by the National Science Centre (Poland) grant number 2022/47/D/ST2/03087. FF acknowledges support from the DFG Research Training Group "GRK 2149: Strong and Weak Interactions — from Hadrons to Dark Matter" and from the German Research Foundation (DFG) under grant number STO 876/4.

References

[1] M. Heikinheimo, M. Kellerstein and V. Sanz, *How Many Supersymmetries?*, *JHEP* **04** (2012) 043 [1111.4322].

[2] P. Diessner, W. Kotlarski, S. Liebschner and D. Stöckinger, *Squark production in R-symmetric SUSY with Dirac gluinos: NLO corrections*, *JHEP* **10** (2017) 142 [1707.04557].

[3] C. Borschensky, F. Frisenna, W. Kotlarski, A. Kulesza and D. Stöckinger, *Squark production with R-symmetry beyond NLO at the LHC*, *JHEP* **05** (2024) 151 [2402.10160].

[4] P. Diessner, J. Kalinowski, W. Kotlarski and D. Stöckinger, *Confronting the coloured sector of the MRSSM with LHC data*, *JHEP* **09** (2019) 120 [1907.11641].

[5] P. Fayet, *Supergauge invariant extension of the Higgs mechanism and a model for the electron and its neutrino*, *Nuclear Physics B* **90** (1975) 104.

[6] A. Salam and J. Strathdee, *Supersymmetry and fermion-number conservation*, *Nuclear Physics B* **87** (1975) 85.

[7] G.D. Kribs, E. Poppitz and N. Weiner, *Flavor in supersymmetry with an extended R-symmetry*, *Phys. Rev. D* **78** (2008) 055010 [0712.2039].

[8] P. Dießner, J. Kalinowski, W. Kotlarski and D. Stöckinger, *Higgs boson mass and electroweak observables in the MRSSM*, *JHEP* **12** (2014) 124 [1410.4791].

[9] P. Diessner, J. Kalinowski, W. Kotlarski and D. Stöckinger, *Two-loop correction to the Higgs boson mass in the MRSSM*, *Adv. High Energy Phys.* **2015** (2015) 760729 [1504.05386].

[10] J. Kalinowski and W. Kotlarski, *Interpreting 95 GeV di-photon/$b\bar{b}$ excesses as a lightest Higgs boson of the MRSSM*, *JHEP* **07** (2024) 037 [2403.08720].

[11] P. Diessner, J. Kalinowski, W. Kotlarski and D. Stöckinger, *Exploring the Higgs sector of the MRSSM with a light scalar*, *JHEP* **03** (2016) 007 [1511.09334].

[12] W. Kotlarski, D. Stöckinger and H. Stöckinger-Kim, *Low-energy lepton physics in the MRSSM: $(g-2)_\mu$, $\mu \to e\gamma$ and $\mu \to e$ conversion*, *JHEP* **08** (2019) 082 [1902.06650].

[13] P. Athron, M. Bach, D.H.J. Jacob, W. Kotlarski, D. Stöckinger and A. Voigt, *Precise calculation of the W boson pole mass beyond the standard model with FlexibleSUSY*, *Phys. Rev. D* **106** (2022) 095023 [2204.05285].